National Aeronautics and Space Administration

FY24 Topic Areas Research and Technology Development (TRTD)

A new method for testing star formation and metal transport theories in galaxies

Principal Investigator: Jorge Luis Pineda Galvez (326)**; Co-Investigators:** William Langer (320), Mathew Orr (Rutgers University/Flatiron Institute)

Strategic Focus Area: Formation and evolution of galaxies

Background: The regulation of star formation in galaxies plays a fundamental role driving galaxy evolution by determining their stellar mass growth and chemical enrichment. Stars form out of the gravitational collapse of dense molecular gas, and, as they form and enter the main sequence, they produce UV and visible photons that can heat and ionize their surroundings, and stellar winds that push accreting material away from the stars. This feedback can reduce the amount of molecular gas available to form additional stars, or, at the very least, reduce the efficiency at which additional stars might form. At later times (>4 Myr) supernova explosions can inject additional energy and momentum, further slowing star formation and destroying their progenitor clouds. These processes together are known as stellar feedback. ***A key unknown in our understanding of the role of star formation in galaxy evolution is the coupling of the energy produced by stellar feedback with its surrounding interstellar medium.*** The distribution of the elemental abundance of nitrogen, which traces metallicity, can be used to determine the efficiency at which energy from stellar feedback is injected into the ISM, and thus we propose that the nitrogen abundance can be used to test competing star-formation theories.

Objectives: The objective of this task is to quantify the energy and momentum that stellar feedback has injected into the ISM of Galactic star forming regions to test competing star formation hypotheses. This objective will be accomplished by obtaining Hydrogen RRL (H-RRL) measurements, which provide the ionizing and kinetic energy of the gas, in a statistically significant sample of Galactic star forming regions covering a range of masses, luminosities, and evolutionary stages. In the program proposed here we will combine the H RRL measurements with archival [NII] observations in the Carina region to provide the first quantitative assessment of the two competing star formation hypotheses using the nitrogen abundance distribution.

Approach and Results: During FY24 we completed the H-RRL mapping as shown in **Figure 1.** We combined archival ISO and SPIFI data to determine the volume and column densities of low and high ionized gas in the Carina Nebula. We find an extended highly ionized component with N^{++} and O^{++} present with electron densities of about 300 cm^{-3}. A low ionization component with only $N^{+\wedge}$ is also present with electron densities of 30-150 cm^{-3}. H^+ and N^+ column densities peak at the location of the stellar cluster in Carina II (**Figure 2**). We also studied the contribution from doubly ionized nitrogen in this region finding that it is the highest near the stellar clusters in Carina (**Figure 3**). The ratio of the total nitrogen (N^++N^{++}) to ionized hydrogen, the nitrogen abundance, shows a relatively flat distribution with respect to the location of stellar clusters (**Figure 4**). This flat distribution tentatively suggests that stellar feedback is strong enough to distribute newly formed metals in the ISM at relatively short timescales. Future observations of the [OIII] 88μm line are important for characterizing this highly ionized component.

We also derived an electron temperature map in the Carina Nebula using the ratio of the RRL to radio continuum emission. The electron temperature is a key ingredient in the derivation of the Nitrogen abundance distribution. In **Figure 5** we show the distribution of electron temperatures derived across the Carina nebula. We find a temperature range between 3000K and 12000K with a tendency for electron temperature to be higher away from the location of the stellar clusters in Carina I and II. Such difference can be an indication of enhanced cooling near the clusters, which in turn is indicative of an increased metallicity. Because of their different masses Hydrogen and Nitrogen are expected to have different thermal line widths, but the same turbulent component. The difference in line widths can also be used to solve for the electron temperature and turbulent component. We fitted Gaussians for the [NII] and RRL data in a set of positions near Carina II and used their line widths to determine the electron temperature. We derived a temperature range from 7000K-12000K, which is consistent with the electron temperature map derived using the ratio of RRL and radio continuum emission for this region.

Significance/Benefits to JPL and NASA: The work performed in this task will provide a new observational technique that can become an important science driver of the JPL-led PRIMA probe mission, a new mission class recommended by the ASTRO2020 Decadal Survey, and follow up flights of the JPL ASTHROS balloon project, a long duration Antarctic NASA balloon, thus giving JPL a competitive lead for the selection of new far-infrared sub-orbital and orbital missions. It will also strengthen the science case for new technology development in important areas of JPL expertise, such as heterodyne and direct detector systems at far-infrared wavelengths, which will enable velocity resolved observations of large samples of star forming regions, and sensitive observations of the disk of large numbers of galaxies, respectively. The proposed work will also showcase the use of the DSN antennas for radio astronomy to support JPL-led NASA missions.

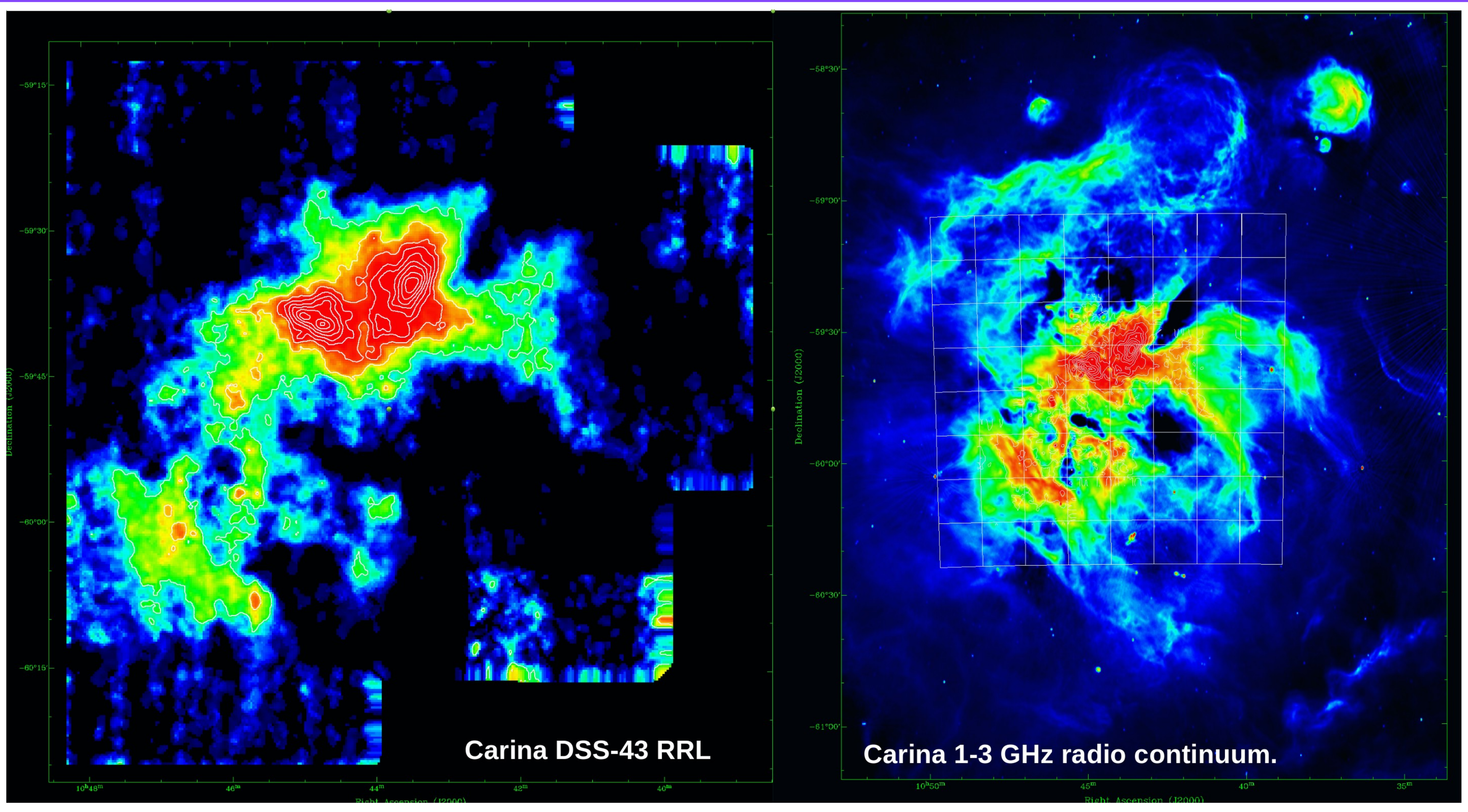

Figure 1: (left) Carina Nebula Observed in Hydrogen RRL with the DSN/DSS-43 antenna. (Right) radio continuum image of the Carina nebula. The planned RRL mapping area is shows as white tiles.

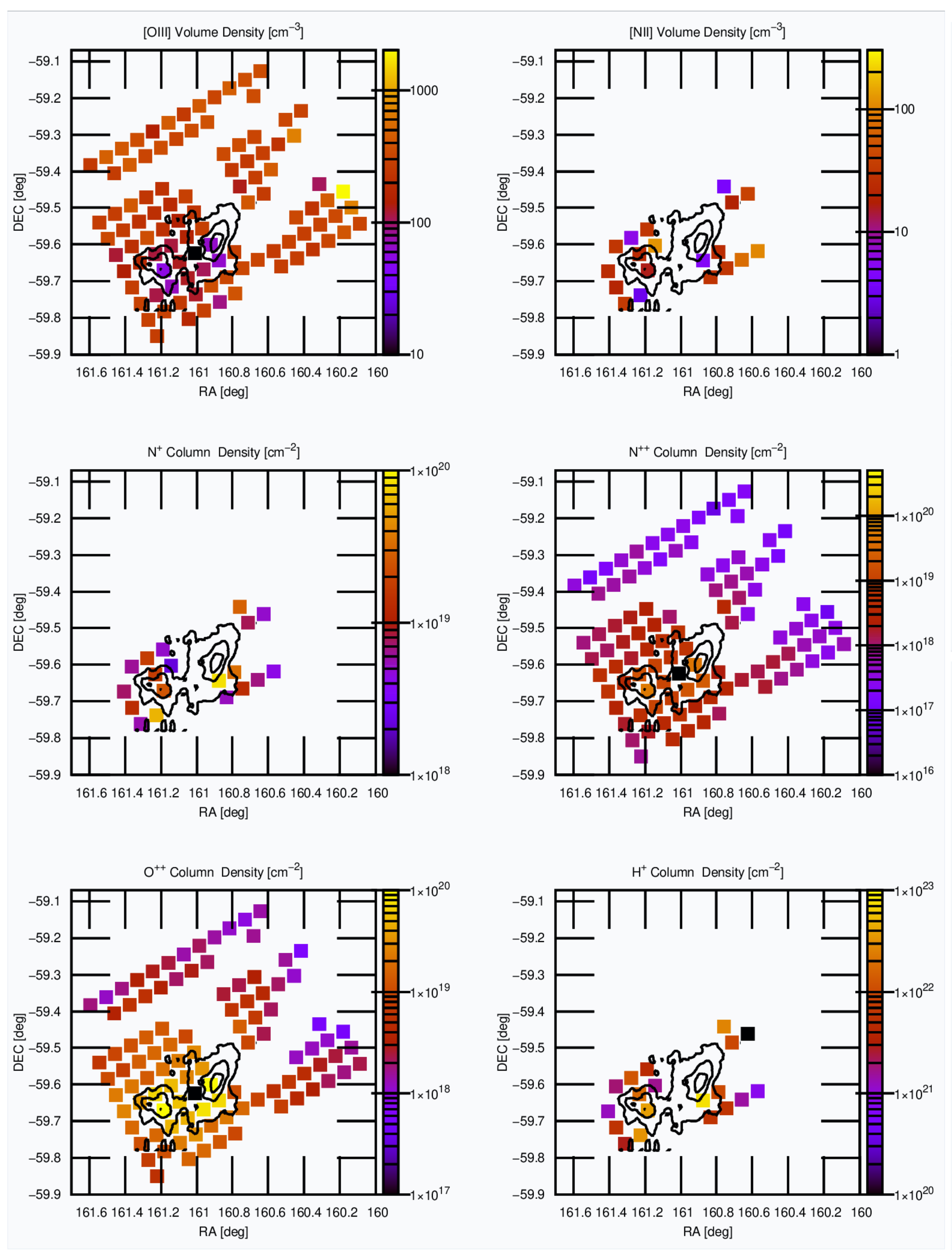

Figure 2: Physical properties derived by combining DSS43 RRL and archival ISO/SOFIA data,

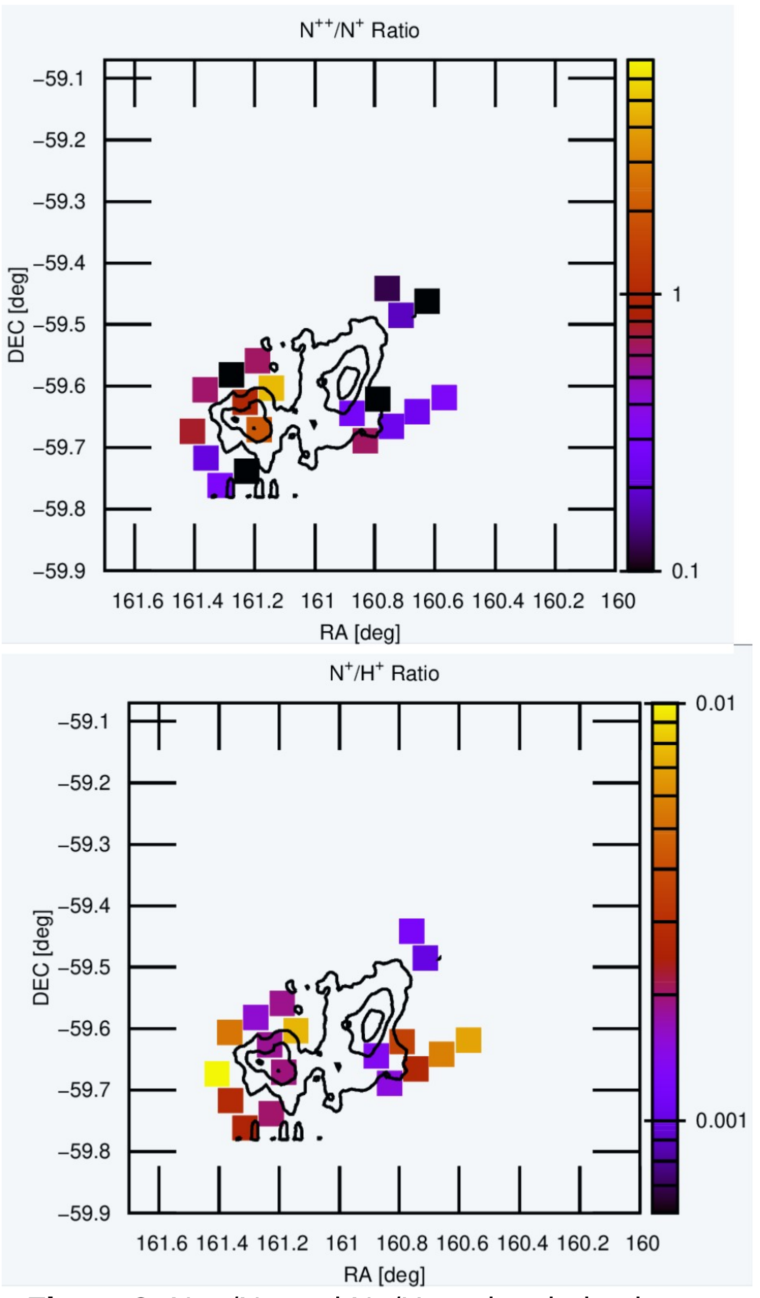

Figure 3: N++/N+ and N+/H+ ratios derived near the Carina I and II stellar clusters

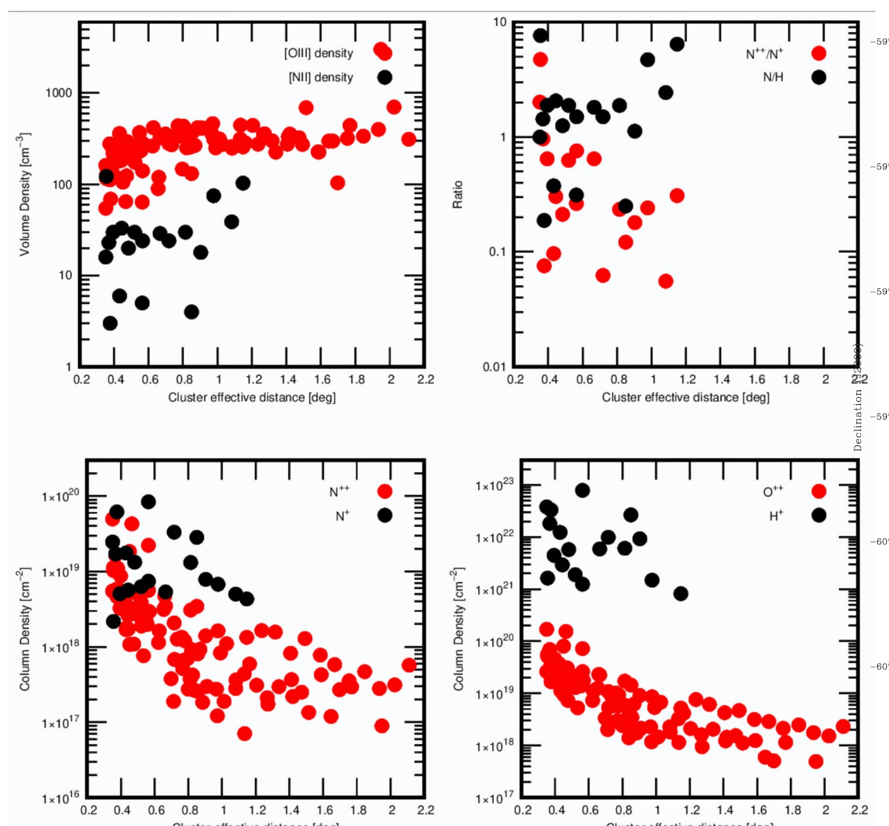

Figure 4: Distribution of different physical properties of the gas in Carina as a function of the effective distance to the Carina I and II stellar clusters.

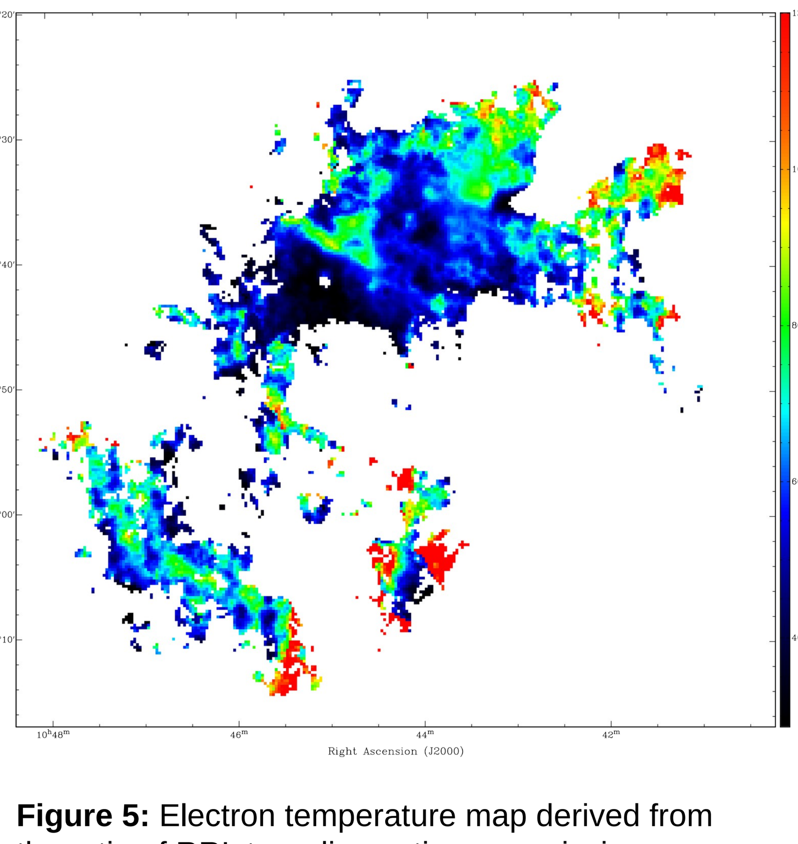

Figure 5: Electron temperature map derived from the ratio of RRL to radio continuum emission.

National Aeronautics and Space Administration

Jet Propulsion Laboratory
California Institute of Technology
Pasadena, California

www.nasa.gov

Publications:

PI/Task Mgr. Contact Information:
626-372-3477 Jorge.Pineda@jpl.nasa.gov